J. Fluid Mech. (1982), *vol.* 114, *pp.* 1–26
Printed in Great Britain

On relating Eulerian and Lagrangian velocity statistics: single particles in homogeneous flows

By RUSS E. DAVIS

Scripps Institution of Oceanography, La Jolla, California 92093

(Received 17 April 1980 and in revised form 9 March 1981)

Various theories seeking to relate the velocity statistics of Lagrangian particles to the statistics of the Eulerian flow in which they are embedded are examined. Mean particle drift, mean-square particle velocity and the frequency spectrum of velocity are examined for stationary, homogeneous and joint-normally distributed Eulerian fields. Predictions based on a third-order weak-interaction expansion, the successive approximation procedure of Phythian (1975), the quasi-normal approximation of Saffman (1969), the parametrized model of Saffman (1962), and a new procedure based on a statistical estimator of the kinematic equation are compared with simulations of particle motion in one-dimensional flow. Only the statistical estimator produces both acceptable mean-drift and frequency-spectrum predictions.

1. Introduction

Recent technical advances have led to an increasing number of oceanic velocity observations made using both moored current meters and freely drifting floats. There are various technical requirements affecting selection of the observational method but the most important distinction between these types of observation is that they characterize fundamentally different aspects of the velocity field. Complete observations of either type allow calculation of any quantity found by the other method but limited data obtained in one reference frame cannot generally answer questions which are easily addressed in the other frame.

In this paper the relation between velocity observations made in the Eulerian reference frame (at fixed positions, as obtained from moorings) and Lagrangian observations (made following fluid particles, as obtained from drifting floats) are examined from the statistical point of view. The hope is that such an examination will aid selection of the appropriate technique for a particular task and, eventually, allow the gain of new insight about the ocean from the differences between observations made in the two reference frames. It is unlikely that there is an exact closed-form relation connecting the low-order statistics which can be deduced from limited observations in the two reference frames. Consequently the approach here is to examine a number of theories claiming to give approximate relations and to test these theories in the simplest case of velocity fields which are statistically homogeneous and stationary and, in the Eulerian frame, have joint-normal distributions. The hope is that those theories which perform best in this simplified context will be the best with which to explore the Eulerian–Lagrangian relationship in more realistic velocity fields.

In a stationary and homogeneous field Eulerian statistics can be defined relative

to time, space or ensemble averages which are equivalent and will be denoted here by $\langle\ \rangle$. If the Eulerian velocity prescription is $\mathbf{u}(\mathbf{x}, t)$ the statistics are, for the joint-normal fields of interest here, completely specified by the mean velocity $\langle u \rangle$ which, without loss of generality, will be taken to vanish, and the covariance tensor

$$E_{nm}(\mathbf{x}, t) = \langle u_n(\mathbf{x}_0, t_0)\, u_m(\mathbf{x}_0 + \mathbf{x}, t_0 + t) \rangle, \tag{1a}$$

where $\mathbf{x}_0$ and t_0 are arbitrary and may be used for averaging. The associated wave-number–frequency spectrum Φ is defined by

$$E_{nm}(\mathbf{x}, t) = \int d\mathbf{k} \int d\omega\, \Phi_{nm}(\mathbf{k}, \omega) \cos(\mathbf{k} \,.\, \mathbf{x} + \omega t), \tag{1b}$$

where by convention integration here is over both signs of ω.

The Lagrangian description of motion involves the particle position $\mathbf{r}$, its velocity $\mathbf{v}$, and identification of the particle. Identification is provided by the particle position at the time of deployment, taken here as time $t = 0$. Thus

$$\mathbf{v}(\mathbf{r}_0, t) = \frac{\partial}{\partial t} \mathbf{r}(\mathbf{r}_0, t) = \mathbf{u}[\mathbf{r}(\mathbf{r}_0, t), t]; \quad \mathbf{r}(\mathbf{r}_0, 0) = \mathbf{r}_0. \tag{2}$$

Definition of Lagrangian statistics involves specifying the class over which averages are taken. Apparently the most useful specification is an ensemble average over many particles which were deployed at random. An important concern of this paper is that, even in homogeneous and stationary Eulerian fields, such statistics are not in general stationary. This is a result of the fact that as particles are moved by the flow they tend to sample preferentially particular regions of that flow. The clearest example of this is particles deployed randomly into a field of compressional waves. At the time of random deployment particles are equally likely to be found in high- and low-density regions of the flow. Later, particles tend to remain longer in high-density regions, where they are advected in the direction of phase motion, than in low-density regions where advection is counter to phase propagation. Thus, for example, a long-term time average of particle motion is more representative of properties in regions of parallel phase and particle propagation than of regions of opposite phase and particle motion. As is discussed below, this behaviour also occurs when particles are deployed in particular regions of non-divergent flows. At the time of deployment, statistics of Lagrangian and Eulerian velocities are equivalent, but later statistics like average particle speed and velocity can differ from the Eulerian counterpart. This is not always accounted for in theories of Lagrangian statistics, as will be seen below. Except in pathologically simple flows it can be expected that long after deployment in homogeneous and stationary Eulerian fields the Lagrangian statistics will become stationary; this state of stationary particle statistics is referred to here as the 'long-after-deployment' limit.

The mean Lagrangian velocity is

$$\mathbf{V}(t) = \langle \mathbf{v}(r_0, t) \rangle,$$

where $\mathbf{r}_0$ is arbitrary and averaging can be carried out over deployment ensembles and over $\mathbf{r}_0$. As $t \to \infty$ it is expected that $\mathbf{V}$ will approach a constant value which, in anisotropic fields, may represent a non-zero Stokes drift. This long-after-deployment mean velocity could be obtained by a time average of a single particle's velocity if that average did not include times near $t = 0$.

The time-lagged mean product of a particle's velocity is

$$\tilde{L}_{nm}(t_1, t_2) = \langle v_n(\mathbf{r}_0, t_1)\, v_m(\mathbf{r}_0, t_2)\rangle. \tag{3a}$$

In the long-after-deployment limit, as t_1 and t_2 become large and $\mathbf{V}$ approaches a constant, a time-lagged covariance can be defined by

$$L_{nm}(t_2 - t_1) = \langle v'_n(t_1)\, v'_m(t_2)\rangle = \lim_{t_1 \to \infty} \tilde{L}_{nm}(t_1, t_2) - V_n V_m, \tag{3b}$$

where $\mathbf{v}' = \mathbf{v} - \mathbf{V}$. The Lagrangian frequency spectrum Ψ is then defined by

$$L_{nm}(t) = \int d\omega\, \Psi_{nm}(\omega) \cos \omega t, \tag{3c}$$

where, by convention, integration over both signs of ω is implied. Particularly descriptive subsets of the information in Ψ are the long-after-deployment particle-velocity variances $L_{nn}(0)$ and single-particle dispersion

$$\sigma^2_{nn}(t) = \lim_{t_0 \to \infty} \langle [r'_n(\mathbf{r}_0, t_0 + t) - r'_n(\mathbf{r}_0, t_0)]^2 \rangle \tag{4}$$

$$= 2 \int_0^t dt' \int_0^{t'} dt''\, L_{nn}(t''),$$

where $\mathbf{r}' = \mathbf{r} - \langle \mathbf{r} \rangle$. By analogy with Fickian diffusion, this particle dispersion can be related (Taylor 1921) to an 'eddy diffusivity'

$$\kappa_{nn}(t) = \frac{1}{2} \frac{d}{dt} \sigma^2_{nn}.$$

If the spectrum Ψ is essentially constant for $|\omega| < 1/\tau$ then for $t \gg \tau$ an approximately constant diffusivity

$$\kappa_{nn}(\infty) = \int_0^\infty L_{nn}(t)\, dt = \pi \Psi_{nn}(0)$$

will be obtained. For $t < \tau$ the diffusivity varies and may take negative values. If Ψ does not approach a limit as $\omega \to 0$ then κ can grow without bound.

The diffusivity κ describes the growing uncertainty in the position of a once-located particle. It does not directly describe the tendency of a particle cloud to increase in size unless the cloud is large enough that particle velocities are uncorrelated (Stommel 1949). Description of relative particle motion requires constructs like the 'neighbour' statistics introduced by Richardson (1926). One such statistic is

$$\Delta^2_{nn}(t - t_0, \mathbf{x}) = \langle [r'_n(\mathbf{a}, t) - r'_n(\mathbf{b}, t)]^2 \rangle,$$

where $\mathbf{a}$ and $\mathbf{b}$ denote particles found at t_0 to be separated by $\mathbf{x}$ and t_0 is restricted to being long after deployment. While easily defined, this averaging procedure is difficult to analyse unless the particle statistics are stationary right from the time of deployment. Analysis of multiple-particle statistics is beyond the scope of this paper.

In their ideal form oceanographic drifters are limited by buoyant stability to movement in prescribed surfaces determined by pressure and density. Thus the lateral motion of the drifter is identical with that of a particle in a two-dimensional flow in which $\mathbf{u}(\mathbf{x}, t)$ is equal to the horizontal component of the three-dimensional flow at the same time t, the same lateral position $\mathbf{x}$, and at the depth of the surface of motion. While there are obvious advantages to viewing drifter motion in terms of its two-

dimensional analogue, there are two points deserving note. First, although the three-dimensional flow is non-divergent, the two-dimensional analogue will in general be divergent. Secondly, some of the unique features of the Lagrangian velocity field may result from differences between the true Eulerian velocity and its two-dimensional analogue. As an example of this latter point, recall that half the classical second-order Stokes drift (Phillips 1977, § 3.3) of a particle on the surface of a deep-water gravity wave results because the mean surface velocity differs from the mean velocity at the mean surface; the other half of the Stokes drift results from the particle remaining longer on a crest than on a trough, just as in the sound-wave example discussed above.

The foregoing introduction is intended to meet three objectives: (i) to establish a nomenclature for some statistical constructs useful in describing stationary and homogeneous Eulerian fields and the Lagrangian kinematics associated with them, (ii) to point out that the statistics of particles released at random differ from the statistics of particles selected at random from a population released long before, and (iii) to establish why examination of divergent Eulerian velocity fields is pertinent to the geophysical context.

The remainder of this paper is concerned with developing and testing methods of predicting Lagrangian statistics from Eulerian statistics in the simplest case of particle motion in one-dimensional divergent flows with homogeneous, stationary and joint-normally distributed Eulerian velocity. Particular interest is placed on prediction of the long-after-deployment mean velocity, mean-square speed, and frequency spectrum. The simplified geometry is pertinent to particle motion in sound waves or in two-dimensional flows where particles are confined to a line in which an Eulerian prescription can be devised, such as drifters confined to constant-pressure surfaces in a two-dimensional flow. The simplified context simplifies notation and all theories are extended trivially to multiple dimensions. It is expected that the relative utility of the theories does not depend on dimensionality but, as Kraichnan (1977) has shown, the predictive ability of theories can be strongly dependent on features of the velocity field which are evident only in three dimensions.

In § 2 a number of previously proposed theories pertaining to description of Lagrangian kinematics are reviewed. These may be divided into approaches based on exact averages of approximate solutions to the particle motion kinematics (2) and approaches based on exact solution of equations approximately describing the evolution of statistics (closure models). From a pedagogic point of view it is interesting to note that the fundamental difficulty in this problem is not the nonlinearity of (2) since it can be converted to a linear equation, as is shown in § 2.3. Rather, the problem is simply that, in either form, this equation cannot be solved exactly and consequently accurate averages of the solution are difficult to obtain.

In § 3 a new approach to the theoretical problem is advanced. The point of novelty here is that a combination of approximate solution of (2) and a statistical hypothesis is employed. The particular theory developed in § 3 may not be adequately developed but it would appear that the concept of combining approximate solutions with closure hypotheses may hold promise over using either alone, in both the present problem and more complex ones.

In § 4 the results of numerical simulations of one-dimensional particle motion are described and compared with the various theories. The primary points of comparison

are the mean Lagrangian drift V, the mean-square particle speed $L(0)$, and the single-particle frequency spectrum $\Psi(\omega)$. Examination of multi-particle statistics, multi-dimensional flow, and inhomogeneous Eulerian fields is deferred.

2. Some previous approaches

Only a few of the numerous approaches to relating Eulerian and Lagrangian statistics are considered here. Those discussed were selected by the criteria that they be based on simple and broad physical principles, that they do not involve adjustable constants, and that they result in Eulerian–Lagrangian relations which are easily evaluated. The latter criterion is imposed because the aim here is not only to evaluate predictive abilities but to expose how features in one reference frame are manifested in the other. Developments are presented in the context of one-dimensional flow to simplify notation; all are extended to several dimensions with ease. Restriction to statistically stationary, homogeneous and joint-normally distributed flow is more than a convenience and certain developments depend critically on one or more of these simplifications.

2.1. *Weak interaction*

In direct analogy to the methods employed to study weakly nonlinear wave fields (Hasselman 1966), description of particle motion can be approached using an expansion in a small parameter ϵ characterizing the ratio of typical particle velocities to typical phase velocities in the Eulerian field. Advantages of this approach are simplicity of the analytical framework already familiar in wave dynamics and the fact that restriction to homogeneous, stationary and joint-normally distributed fields is not essential. Disadvantages are that predictive ability is limited to very small values of ϵ and that algebraic complexity escalates rapidly with the order to which the analysis is carried. The limited ability to predict Lagrangian behaviour (see § 4) may have implications for the interpretation of wave-interaction theories seeking to describe cross-spectral energy transfer.

The weak-interaction approach is the classical one used to describe particle motion in wave fields (*cf.* Phillips 1977, § 3.3; Kenyon 1969; Hoult 1968). A two-term expansion is sufficient to disclose a difference between the mean Eulerian velocity and the mean Lagrangian velocity V, and this same analysis clearly demonstrates how the transition to the statistically stationary 'long-after-deployment' limit of Lagrangian motion is achieved. To my knowledge the approach has not previously been carried to the point where changes between the Eulerian and Lagrangian frequency spectra are detectable, but this involves only a routine calculation.

Let length and time be normalized by the characteristic scales of the Eulerian spectrum and take

$$\begin{aligned} u(x,t) &= \epsilon\hat{u}(x,t), \\ v(t) = v(t;0) &= V(t)+\epsilon\hat{v}_1(t)+\epsilon^2\hat{v}_2(t)+\ldots, \\ r(t) = r(t;0) &= R(\tau)+\epsilon\hat{r}_1(t)+\epsilon^2\hat{r}_2(t)+\ldots, \end{aligned}$$

where $\tau = \epsilon^2 t$ is a slow time over which the particle may drift a distance of order unity; the dependence of v_n and r_n on τ is not denoted explicitly. $V(t)$ is the mean Lagrangian

velocity obtained by averaging over realizations of the Eulerian flow. A conventional two-time expansion, which rests essentially on the Taylor series

$$u(r,t) = \epsilon\hat{u}(R,t) + \epsilon^2\hat{r}_1(t)\,\hat{u}_x(R,t) + \ldots,$$

has been carried to determination of v_3.

At $O(\epsilon^2)$ the mean Lagrangian drift velocity

$$V(t) = \epsilon^2\langle\hat{u}_x(R,t)\,\hat{r}_1(t)\rangle = \int_0^t E_x(0,t')\,dt' \tag{5}$$

is obtained. So long as the Eulerian spectrum is finite at zero frequency this velocity, essentially a Stokes drift, approaches a constant for long times after initial random deployment. From the definition

$$V(t) = \langle u\{r(t),t\}\rangle$$

it is obvious that $V(0) = 0$ since $r(0)$ is the random deployment position. In anisotropic velocity fields a correlation of particle position and velocity develops during a transition period, leading to a non-zero V.

An approximation of $\langle v(t_1)\,v(t_2)\rangle = \tilde{L}(t_1,t_2)$ to $O(\epsilon^4)$ can be achieved with the restriction that the Eulerian spectrum vanish at zero frequency. This is required so that $\langle r_1^2\rangle$ remain bounded and the restrictions of the expansion not be violated. Then the approximation

$$\begin{aligned}\langle v(t_1)\,v(t_2)\rangle = {} & \langle u(t_1)\,u(t_2)\rangle + \langle u_x(t_1)\,u_x(t_2)\,r_1(t_1)\,r_1(t_2)\rangle \\ & + \tfrac{1}{2}\langle u(t_1)\,u_{xx}(t_2)\,r_1^2(t_2) + u(t_2)\,u_{xx}(t_1)\,r_1^2(t_1)\rangle \\ & + \langle u(t_1)\,u_x(t_2)\,r_2(t_2) + u(t_2)\,u_x(t_1)\,r_2(t_1)\rangle,\end{aligned}$$

$$r_1(t) = \int_0^t u(t')\,dt', \quad r_2(t) = \int_0^t \left[u_x(t')\,r_1(t') - \frac{dR(\epsilon^2 t')}{dt'}\right]dt',$$

where $u(t)$ denotes $u\{R(\epsilon^2 t),t\}$, can be directly evaluated for joint-normally distributed $u(x,t)$. In terms of the Eulerian covariance the result is, to $O(\epsilon^4)$,

$$\begin{aligned}\tilde{L}(t_1,t_2) = {} & E(\langle R_2 - R_1\rangle, t_2 - t_1) + \tfrac{1}{2}E_{xx}(t_2-t_1)\langle\{r_1(t_2) - r_1(t_1)\}^2\rangle \\ & + \int_0^{t_1} E_x(t'-t_2)\,dt' \int_0^{t_2} E_x(t'-t_1)\,dt' \\ & + \left[\int_0^{t_1} E(t'-t_2)\,dt' \int_0^{t_1} E_{xx}(t'-t_1)\,dt'\right] + [*] \\ & - \left[\int_0^{t_1} dt' \int_0^{t'} \{E_x(t'-t_2)\,E_x(t''-t_1) + E_{xx}(t'-t_1)\,E(t''-t_2)\}\right] - [*],\end{aligned} \tag{6}$$

where

$$\langle R_n\rangle = \int_0^{t_n} V(t)\,dt,$$

$E(t)$ denotes $E(0,t)$, the symbol $[*]$ denotes the $[\ ]$ expression to the left with t_1 and t_2 interchanged, and

$$\langle\{r_1(t_2) - r_1(t_1)\}^2\rangle = \int_{t_1}^{t_2} dt' \int_{t_1}^{t_2} dt''\,E(t''-t').$$

The point of greatest importance here is that $\langle v(t_1)\,v(t_2)\rangle$ is a function of t_1 and t_2 until

both become large and stationary Lagrangian statistics are achieved; this feature of the approximation is borne out well in simulation experiments.

In the long-after-deployment limit $\tilde{L}(t_1, t_2) - V^2$ becomes a function of $t = t_1 - t_2$ alone, being

$$\begin{aligned} L(t) = E(Vt, t) + E_{xx}(0,t)\,[H(0,0) - H(0,t)] + H_{xt}^2(0,t) \\ + \int_{-\infty}^{0} dt'\, E_{xx}(0,t')\,[H_t(0, t+t') - H_t(0, t-t')] \\ + \int_{-\infty}^{0} dt'\, H_{xt}(0,t')\,[E_x(0,t+t') - E_x(0,t-t')], \end{aligned}$$

where

$$H(x,t) = -\int_{-\infty}^{t} dt' \int_{-\infty}^{t'} dt''\, E(x,t'')$$

is the covariance $\langle r_1(x,t)\, r_1(0,0)\rangle$. The Lagrangian frequency spectrum is easily computed from $L(t)$ and in the special case of isotropic Eulerian fields, where $V = 0$, is

$$\begin{aligned} \Psi(\omega) = \int dk\, \Phi(k,\omega) \left[1 + \mathscr{P} \int d\omega_1\, dk_1\, \Phi(\omega_1, k_1) \left\{\frac{2k_1^2}{\omega_1^2 - \omega^2} - \frac{k^2}{\omega_1^2}\right\}\right] \\ + \int dk \int dk_1\, d\omega_1\, \Phi(\omega_1, k_1) \frac{k^2}{\omega_1^2} \tfrac{1}{2}\{\Phi(\omega - \omega_1, k) + \Phi(\omega + \omega_1, k)\}, \end{aligned} \tag{7}$$

where $\mathscr{P}$ denotes Cauchy's principal value excluding $\omega_1^2 = \omega^2$ and Φ is the Eulerian wavenumber–frequency spectrum.

2.2. *Successive approximation*

The weak-interaction approach rests, in the final analysis, on a Taylor-series expansion of the Eulerian velocity around some location near where the Lagrangian particle is located. Restricting the Eulerian field to have no energy at zero frequency and velocities small compared with typical phase velocities permits the expansion, at least as an asymptotic limit. Phythian (1975) has suggested a related approach, based on successive approximations, which at least formally is not limited to small particle displacements. Phythian considered only isotropic, stationary, homogeneous fields and showed that the second approximation is easily evaluated for joint-normally distributed fields. Relaxation of any or all of these restrictions appears possible but computational effort threatens to escalate quickly.

The successive approximation scheme is based on the recurrence relation

$$r_{n+1}(t) = \int_0^t u\{r_n(t'), t'\}\, dt'.$$

With the initial approximation $r_0(t) = 0$ one obtains

$$r_1(t) = \int_0^t u(0,t')\, dt',$$

$$v_2(t) = \frac{dr_2(t)}{dt} = u(r_1(t), t).$$

Failing to account for the non-stationary behaviour of the Lagrangian statistics, Phythian suggested the approximation

$$L(t) \simeq \langle v_2(0)\, v_2(t)\rangle = \int dx \langle u(0,0)\, u(x,t)\, \delta\{x - r_1(t)\}\rangle$$

$$= \frac{1}{2\pi}\int dk \int dx \exp(ikx) \langle u(0,0)\, u(x,t) \exp\{-ikr_1(t)\}\rangle$$

$$= \frac{1}{2\pi}\int dk \int dx \exp(ikx) \left[\frac{\partial}{\partial\alpha}\frac{\partial}{\partial\beta} z(x,t;\alpha,\beta)\right]_{\alpha=\beta=0},$$

where

$$z = -\langle \exp[i\{-kr_1(t) + \alpha u(0,0) + \beta u(x,t)\}]\rangle.$$

Because r_1 is a linear operation on the joint-normally distributed Eulerian velocity, the exponent in the expression for z is normally distributed and the expectation value can be obtained analytically, yielding

$$L(\tau) = \frac{1}{2\pi}\int dk \int dx \exp\{ikx - \tfrac{1}{2}k^2\sigma_1^2(\tau)\}\, [\langle u(0,0)\, u(x,\tau)\rangle - k^2 \langle r_1(\tau)\, u(0,0)\rangle \langle r_1(\tau)\, u(x,\tau)\rangle]$$

$$= \int dx\, [\{2\pi\sigma_1^2\}^{-\frac{1}{2}} \exp\{-x^2/2\sigma_1^2\}] \left[E(x,\tau) - \frac{1}{\sigma_1}\frac{d\sigma_1}{dt}\left\{1 - \frac{x^2}{\sigma_1^2}\right\}\int_0^\tau E(x,t)\, dt\right], \tag{8}$$

where

$$\sigma_1^2(\tau) = \langle r_1^2(\tau)\rangle = \int_0^\tau dt' \int_0^\tau dt''\, E(0, t' - t'').$$

For subsequent reference, note that the last term of (8), involving an integral of E, results from correlation of r_1 and u; the first term, involving the exponential, will be recognized as the Gaussian distribution of $x - r_1$ or, equivalently, the concentration of marked particles at position x.

Extending the same expansion and methodology to determining mean Lagrangian drift, one obtains

$$V(t) = \int dx \langle u(x,t)\, \delta[x - r_1(t)]\rangle$$

$$= \int dx\, [\{2\pi\sigma_1^2\}^{-\frac{1}{2}} \exp\{-x^2/2\sigma_1^2\}] \int_0^t E_x(x,t')\, dt'$$

$$= \int dx\, \{2\pi\}^{-\frac{1}{2}} \exp\{-\tfrac{1}{2}x^2\} \int_0^t E_x(x\sigma_1, t')\, dt'. \tag{9}$$

It is interesting to note that this expression for $V(t)$ is consistent with that obtained from the weak-interaction theory under the conditions where the latter applies. Note that σ_1^2 is the variance of $r_1(t)$, not of the full $r(t)$, so that if the Eulerian spectrum contains no energy at zero frequency σ_1 approaches a finite limit as $t \to \infty$. If $E(x,t)$ is $O(\epsilon^2)$, as in the weak-interaction approach, then σ_1 is $O(\epsilon)$ and (9) may be expanded in powers of ϵ yielding (5) as the leading term. On the other hand (9) also applies to Eulerian fields with finite energy at zero frequency, in which case σ_1 grows without bound and the predicted V vanishes. Phythian suggested that when $V \neq 0$ the selection $r_0 = 0$ may be inappropriate but changing r_0 does not appear to alter the basic behaviour of $V(t)$, specifically the prediction that V vanishes as σ_1 becomes large. The simulations of § 4 show this prediction to be incorrect.

2.3. *Quasi-normal approximation*

Both the theories outlined above are based on approximate solutions of the fundamental kinematic equation (2), written in its nonlinear form. Thus they are based on exact averages of approximate solutions of the problem. An alternative approach, more in line with the 'closure theories' used in modelling turbulence, is to seek approximate equations which describe the evolution of statistics and which can be solved exactly. As an example, the quasi-normal approximation first introduced by Saffman (1969) will be discussed; it is the simplest of a category of theories based on predicting the probability distribution of particle position.

That the difficulty in solving the kinematic equation (2) is not its nonlinearity is demonstrated by converting it to the 'advected scalar' equation

$$c(x,t) = \delta[x - r(t)], \quad \partial_t c + \partial_x uc = 0. \tag{10}$$

Here $c(x,t)$ is the analogue of concentration per unit length (volume in three dimensions) of marked particles and δ is the Dirac delta function. By considering an ensemble of realizations for which $c(0,0) = \delta(x)$ one can decompose the concentration into a mean component C and a fluctuation c' such that $\langle c' \rangle = 0$.

The Weiner–Hermite expansion employed by Saffman (1969) is equivalent to the quasi-normal approximation that the moment $\langle uuc' \rangle$ vanishes. The virtue of the Weiner–Hermite expansion is that it can, in principle, be carried to higher order so that non-vanishing cumulants can eventually be included. The higher-order expansion has not yet been implemented so the outline here follows the simpler quasi-normal framework. Thus the mean and fluctuating parts of the advected scalar equation are

$$\partial_t C + \partial_x \langle uc' \rangle = 0,$$

$$c'(x,t) = -\partial_x \int_0^t dt' \, [u(x,t')\{c'(x,t') + C(x,t')\} - \langle u(x,t')\, c'(x,t') \rangle].$$

Substituting c' into the equation for C and dropping $\langle uuc' \rangle$ gives

$$\begin{aligned} \partial_t C &= \int_0^t dt' \, \partial_x \langle u(x,t)\, \partial_x \{u(x,t')\, C(x,t')\} \rangle \\ &= \int_0^t dt' \, [E(0,t'-t)\, \partial_{xx}^2 C(x,t') + E_x(0,t'-t)\, \partial_x C(x,t')]. \end{aligned} \tag{11}$$

The quasi-normal approximation also leads to a simple relation for the Lagrangian covariance if the non-stationary Lagrangian behaviour following deployment is ignored; thus

$$L(t) + V^2 \simeq \tilde{L}(t,0) = \int dx \, \langle u(0,0)\, u(x,t)\, c(x,t) \rangle$$

with the quasi-normal approximation yields

$$L(t) = \int dx \, E(x,t)\, C(x,t) - V^2. \tag{12}$$

The approximation (12), where C is the true mean concentration, not that given by (11), was first advanced by Corrsin (1960). It plays a central role in various theories of turbulent dispersion including Kraichnan's direct-interaction approximation. Corrsin's conjecture (12) corresponds to dropping all but the first two terms of the

weak-interaction approximation (6) and neglecting the second term of (8) for the successive-approximation procedure.

The mean drift predicted by the quasi-normal approximation is identical to (5) obtained from weak-interaction theory. This is shown when (11) is substituted into

$$V = \frac{d}{dt}\int xC(x,t)\,dx,$$

which is then integrated by parts to obtain

$$V = -\int_0^t dt'\,E_x(0,t'-t)\int C(x,t')\,dx = \int_0^t E_x(0,t')\,dt'. \tag{13}$$

The mean concentration predicted by (11) has some unrealistic features which can most easily be discussed for isotropic fields when $E_x(0,t) = 0$. A small-time expansion of (11) then yields

$$\partial_{tt}C = E(0,0)\,\partial_{xx}C + O(t^2),$$

indicating that the mean concentration initially behaves as a non-dispersive wave propagating at the root-mean-square Eulerian velocity. This physically unrealistic behaviour will be implicated in comparisons of observed and predicted Lagrangian covariances.

2.4. *Direct-interaction approximation*

The direct-interaction approximation (DIA), introduced by Kraichnan (1959), has been applied to prediction of Lagrangian velocity statistics by Roberts (1961) and those predictions were tested by Kraichnan (1970). Evaluation of the DIA predictions rivals in computational difficulty direct simulation of particle motion; the more advanced DIA adaptations predicting Lagrangian statistics by Kraichnan (1965, 1977) would involve even more extensive computation. Consequently, the DIA is not tested here and discussion is limited to some general features of the unaltered DIA.

Working from the scalar concentration equation (10), Roberts obtained an equation describing evolution of the mean concentration resulting from the initial condition $C(x,0) = \delta(x)$. Repeating his derivation (equations (2.31–2.43)) without the restriction of incompressible flow leads to

$$\partial_t C(\mathbf{x},t) = \int_0^t dt'\int dy\,E_{nm}(\mathbf{y},t')\frac{\partial}{\partial y_m}G(\mathbf{y},t')\frac{\partial}{\partial x_n}G(\mathbf{x}-\mathbf{y},t-t'). \tag{14}$$

The evolution model is non-local in time (like the quasi-normal approximation) and in space; the nonlinearity is consistent with the linear nature of (10) because (14) pertains only to the initial condition $C(\mathbf{x},0) = \delta(\mathbf{x})$.

Because the DIA evolution conserves mass, that is $\int d\mathbf{x}\,C(\mathbf{x},t) = 1$, Lagrangian velocity is easily found, through integration by parts, to be

$$V_n(t) = \int d\mathbf{x}\,x_n\,\partial_t C = \int_0^t dt'\int d\mathbf{x}\,C(\mathbf{x},t)\frac{\partial}{\partial x_m}E_{nm}(\mathbf{x},t).$$

In the limit of weak motions, when $C(x,t)$ approximates $\delta(x)$ for large times, the DIA prediction for $V(t)$ is the same as (5) from weak-interaction theory and (13) from the quasi-normal approximation. In multi-dimensional flow existence of non-zero mean Lagrangian velocity requires both compressible flow and anisotropic Eulerian statistics.

In incompressible flows the Lagrangian statistics are stationary, there is no mean Lagrangian velocity, and, as Roberts showed, the Lagrangian covariance predicted by the DIA is

$$L(t) = \int dx\, E(x,t)\, C(x,t),$$

which will be recognized as Corrsin's conjecture (12). When the flow is compressible, as in the case considered here, the Lagrangian covariance cannot be deduced from $C(x,t)$. The mean product of Lagrangian velocities at two times is

$$\begin{aligned}\langle v(t)\, v(s)\rangle &= -\tfrac{1}{2}\partial_s\partial_t\langle[r(x_0,t)-r(x_0,s)]^2\rangle \\ &= -\tfrac{1}{2}\partial_s\partial_t\int dx\, dy\,(x-y)^2\langle c(x,t)\, c(y,s)\rangle \\ &= -\partial_s\partial_t\int dx\, \tfrac{1}{2}x^2\, R(x,t,s),\end{aligned}$$

where

$$R(x,t,s) = \int dy\, \langle c(x+y,s)\, c(y,t)\rangle.$$

Here $R(x,t,s)$ is the same as $R(x,t,s\,|\,0,0,0)$ considered in § 3.2 of Roberts (1961). If his derivation of the evolution equation for R is repeated without the constraint of incompressible flow, one obtains

$$\begin{aligned}\partial_t R(\mathbf{x},t,s) = {} & \frac{\partial}{\partial x_n}\int d\mathbf{x}'\int_0^t dt'\, C(\mathbf{x}',t')\, R(\mathbf{x}+\mathbf{x}',t-t',s)\frac{\partial}{\partial x_m'}E_{nm}(\mathbf{x}',t') \\ & + \frac{\partial^2}{\partial x_n\,\partial x_N}\int d\mathbf{x}'\left\{\int_0^t dt'\, E_{nm}(\mathbf{x}',t')\, C(\mathbf{x}',t')\, R(\mathbf{x}+\mathbf{x}',t-t',s)\right. \\ & \left. - \int_0^s ds'\, E_{nm}(\mathbf{x}-\mathbf{x}',s-t-s')\, C(\mathbf{x}',s')\, R(\mathbf{x}-\mathbf{x}',t,s-s')\right\}.\end{aligned}$$

The first term vanishes for incompressible flow and the last two terms correspond to Roberts' (3.25). If this is used to evaluate the time-lagged mean product of Lagrangian velocity one finds, after some manipulation,

$$\langle v(t)\, v(s)\rangle = V(t)\, V(s) + \int dx\, E(x,s-t)\, R(x,t,s).$$

Without solving for R it is possible only to note that, since $R(x,t,t) = \delta(x)$, the DIA predicts

$$L(0) = \langle v^2(t)\rangle - V^2 = E(0,0),$$

that is, that Lagrangian and Eulerian velocity variances are equal. This is not found to be the case in the simulations described below.

2.5. *Parametrized Gaussian model*

Both the quasi-normal approximation of § 2.3 and the DIA of § 2.4 invoke two results in order to obtain the Lagrangian velocity covariance. Each involves an evolution equation for the mean concentration of particles (different for the two theories) and a method of using the resulting probability distribution of particle position to find the Lagrangian covariance (using Corrsin's conjecture (12) for both).

Saffman (1962) has shown that, if (12) is accepted and the shape of the mean concentration field is specified, then a much simplified concentration evolution equation is achieved. Presumably on the basis of observational suggestions such as those quoted by Hinze (1959), Saffman proposed for isotropic fields that the mean concentration has a Gaussian shape so that for one-dimensional flow

$$C(x,t) = \frac{1}{\sqrt{(2\pi)}}\frac{1}{\sigma}\exp\left(-\frac{x^2}{2\sigma^2}\right),$$

where by definition $\sigma^2 = \langle r^2 \rangle$. From (4) and (12) it follows that σ^2 evolves according to

$$\frac{1}{2}\frac{d^2}{dt^2}\sigma^2 = L(t) = \int C(x,t)\,E(x,t)\,dx, \tag{15}$$

which is much more easily solved than the evolution equations of §§ 2.3, 2.4. It should be noted that the successive approximation theory also approximates C with a Gaussian shape but does not employ Corrsin's conjecture (12). While a Gaussian shape for C is consistent with Fickian diffusion it does not imply Fickian diffusion unless $\sigma^2 = 2\kappa t$, where κ is a constant. For sufficiently large times, when σ is much larger than the correlation length of $E(x,t)$ or t is much larger than the correlation time, Saffman's model approaches this limiting form, a feature in accord with simulations.

The Gaussian parametrization approach does not permit prediction of mean Lagrangian drifts in anisotropic fields. The Gaussian model itself is easily modified to account for a moving mean particle position, but the mean position cannot be predicted from the resulting model. The reason for this can be understood when it is noted that $C(x,t)$ addresses the probability of finding near (x,t) a particle released at $(0,0)$ given no information beyond the values (x,t). Since the Lagrangian drift results from a correlation of Eulerian velocity and particle position it is not surprising that the drift cannot be determined from a probability density which considers only position.

In § 3 we take up a new approach to prediction of Lagrangian velocity statistics which in its simplest form reduces to the parametrized Gaussian model but is capable of extension to prediction of Lagrangian drift.

3. The statistical-estimator approach

Review of the theories summarized in § 2 shows that they may be classified into two groups according to their fundamental approach. The weak-interaction and successive-approximation theories of § 2.1 and § 2.2 are based on exact averages of approximate solutions of the fundamental kinematic equation (2). The quasi-normal closure, direct interaction approximation and parametrized Gaussian models of § 2.3, § 2.4 and § 2.5 are, in contrast, based on solving exactly an equation hypothesized to describe the evolution of statistical quantities. The former category suffers from the practical necessity of limiting analysis to approximate solutions which are simple and therefore inaccurate. The latter category suffers from an intrinsic lack of fundamental principles to use in establishing statistical relations. A unique element of the approach described here is incorporating into the fundamental kinematical equations a statistical estimator which blends statistical hypothesis with approximate mathematics. An additional feature is that account is taken of the difference between randomly deployed particles and particles selected at random long after their deployment.

3.1. *Long-after-deployment statistics*

As pointed out in § 2, stationary Lagrangian statistics are achieved only after deployment. During the transition to this statistically stationary state, statistical relations develop between particle velocity and position. In order to deal with these relations, which occur in both divergent and nondivergent flows, it is convenient to

introduce a set of Lagrangian co-ordinates $\mathbf{m}$ which remain fixed along a particle trajectory. A fluid 'parcel' is then the infinitesimal element $|d\mathbf{m}|$ and conservation of mass requires that the linear dimensions of the parcel obey $|dm| = \rho\,|dx|$ where ρ obeys

$$\partial_t \rho + \nabla . \mathbf{u}\rho = 0. \tag{16}$$

Long after deployment statistics apply to ensembles of particles initially deployed randomly over some region $\mathscr{M}$ of the fluid which then defines the region over which averages are to be taken. As an example, consider surface wave motion confined to two dimensions in which the statistics of surface particle motion are of interest. One approach is to define $\mathscr{M}$ as a thin material area near the surface in which, if the two-dimensional flow is non-divergent, ρ is constant. An alternative is to define a material line, M, which is confined to the surface itself but in which ρ, the mass per unit length of particles, varies because the tangential component of surface flow is divergent.

The long-after-deployment limit of the mean Lagrangian velocity is obtained by averaging over the material element $\mathscr{M}$. Thus

$$\mathbf{V} = \int_{\mathscr{M}} \mathbf{u}\{\mathbf{x}(\mathbf{m},t),t\}\,d\mathbf{m} \Big/ \int_{\mathscr{M}} d\mathbf{m}$$

since the particles of interest are uniformly distributed in $\mathbf{m}$-space. If $\mathscr{A}$ is the area in $\mathbf{x}$-space occupied by $\mathscr{M}$, then using $d\mathbf{m} = \rho d\mathbf{x}$ one obtains

$$\mathbf{V} = \int_{\mathscr{A}} \rho(\mathbf{x},t)\,\mathbf{u}(\mathbf{x},t)\,d\mathbf{x} \Big/ \int_{\mathscr{A}} \rho(\mathbf{x},t)\,d\mathbf{x}. \tag{17}$$

Consider now the surface wave example above. If M is a line along the surface then A is the line length, and (17) becomes $\mathbf{V} = \langle \rho\mathbf{u}\rangle / \langle\rho\rangle$, where $\langle\ \rangle$ is the average along the line M. With the two-dimensional definition of $\mathscr{M}$, ρ is constant, and the area $\mathscr{A}$ is itself modulated by the flow. If p, the thickness of the thin region $\mathscr{A}$, is sufficiently small, then (17) becomes $\mathbf{V} = \langle p\mathbf{u}\rangle / \langle p\rangle$ with the same meaning of $\langle\ \rangle$. The result of either approach is the same; in one case convergence of the tangential surface flow is reflected in a changing density, in the other case it is reflected in a deformation of the averaging area. In either case Lagrangian drift results because the particles being followed are found preferentially on wave crests since both ρ and p are greater there.

The Lagrangian time-lagged mean product is determined in the same way, leading to

$$\langle v(t)\,v(t+\tau)\rangle = \int_{\mathscr{A}} \rho\{\mathbf{x},t\}\,\mathbf{u}\{\mathbf{x},t\}\,\mathbf{u}\{\mathbf{r}(\tau)+\mathbf{x},\tau+t\}\,d\mathbf{x} \Big/ \int_{\mathscr{A}} \rho\,d\mathbf{x}, \tag{18}$$

where $\mathbf{r}$ is the displacement of the particle found at $\mathbf{x}$ at time t.

Because the Eulerian field is stationary, the integrals in (17) and (18) define average quantities so that, with the definition $\langle\rho\rangle = 1$, we may write for the one-dimensional case

$$V = \langle \rho(x,t)\,u(x,t)\rangle, \tag{19}$$

$$\langle v(t)\,v(t+\tau)\rangle = \langle \rho(x,t)\,u(x,t)\,u(x+r\{\tau\},t+\tau)\rangle. \tag{20}$$

The contrast between (20) and (3) results because (20) pertains to the 'long-after-deployment' limit, in which the probability of finding particles at (x,t) is not

necessarily uniform, whereas (3) pertains to averaging over initial deployments which, by definition, are random and thus equally probable at any position. The virtue of (19) and (20) is that they allow determination of long-after-deployment statistics without requiring knowledge of particle displacement over long times; they are not appropriate for determination of the non-stationary statistics describing behaviour following random deployment.

It must be reiterated that the effect of variable ρ shown in (19) and (20) is not restricted to divergent fields. This is so because ρ is a property of the density field and how the particles over which averages are to be taken were deployed. Thus (19) and (20) apply to both divergent one-dimensional flow and multi-dimensional non-divergent flow in which particles are deployed in a thin tube with axial velocity u and mass per unit length ρ. Similarly description of particles deployed in a thin sheet in a three-dimensional non-divergent flow could be approached through a two-dimensional version of (19) and (20).

3.2. *Statistical estimators*

In the present approach we seek to evaluate (19) and (20) using exact averages (without closure hypotheses) and estimates of ρ and r. The unique feature is that the estimates of ρ and r are made using statistically optimized estimators rather than an expansion procedure such as that employed in the weak-interaction and successive-approximation approaches of § 2.1 and § 2.2. Statistically optimized estimators have been employed extensively in developing empirical predictors for complex fluid-dynamical system (*cf.* Davis 1977) but are less widely applied in theoretical developments. The fundamental philosophy is that certain variables are selected as being pertinent to determining the quantity to be estimated and then these variables are combined in a manner which minimizes a statistical measure of the error of the estimate. The statistical estimation technique and expansion procedures are not necessarily mutually exclusive since expansion solutions can serve to isolate the pertinent variables upon which the statistically optimized estimate is based.

Consider first estimation of the density ρ which obeys the conservation equation

$$(\partial_t + u\partial_x)\ln\rho = -\partial_x u. \tag{21}$$

Analogous to the weak-interaction approach of § 2.1, an expansion in terms of small u would produce the leading term

$$\ln\{\rho(x,t)\} = -\int_{-\infty}^{t} \partial_x u(x,t')\,dt' \equiv -\eta_x(x,t).$$

In the opposite limit, when the advective term of (21) dominates, particles accumulate at points where $u = 0$, $u_x < 0$; examples of this tendency in large-amplitude flow are provided by Liu & Thompson (1974).

In this examination, the statistically optimized density estimator

$$\hat{\rho} = e^{-\alpha\eta_x}[1+\beta u^2]^{\gamma}\rho_0^{-1}, \tag{22}$$

with $\beta > 0$, is explored. The constants α, β and γ are selected to minimize a statistical measure of the error when (22) is substituted in (21) while ρ_0 is selected so that $\langle\hat{\rho}\rangle = 1$. When $\beta = 0$ the estimator becomes the first term in the weak-interaction solution of (21). The term involving β and γ is, frankly, a crude way of modifying the weak-interaction solution to account for the advective term in (21) and permit the modelling

of phenomena such as particle accumulation at points where u is small. The particular form was selected primarily for computational simplicity rather than theoretical inspiration or trial-and-error testing. In essence, the thesis of this examination is that statistical optimization of simple functional forms can lead to accurate results without appeal to phenomenological 'closure hypotheses'.

In terms of the error measure $\epsilon = \ln(\rho/\hat{\rho})$ the constants in (22) are selected to minimize the mean square of the error in (21), which is

$$\frac{d\epsilon}{dt} = u_x - (\partial_t + u\,\partial_x)\ln\hat{\rho}.$$

It is not possible to minimize $\langle\epsilon^2\rangle$ since ρ itself is not known. The functional to be minimized is

$$\left\langle\left(\frac{d\epsilon}{dt}\right)^2\right\rangle = (\alpha-1)^2\langle u_x^2\rangle + \alpha^2\langle u^2\rangle\langle\eta_{xx}^2\rangle + [\gamma^2 + (4\alpha-2)\gamma]\langle u_x^2\rangle[1-B] + \gamma^2[\langle u_x^2\rangle - \beta\langle u_t^2\rangle]\,\beta\frac{dB}{d\beta},$$

where

$$B(\beta) \equiv \langle[1+\beta u^2]^{-1}\rangle.$$

Since u is specified to be normally distributed, $B(\beta)$ can be evaluated analytically in terms of the error function (*cf.* Abramowitz & Stegun 1964). For any particular β, the optimal values of α and γ can be found analytically by the usual procedure of extremizing the quadratic form. The optimal β, however, must be found by an exhaustive search which in practice is simple and economical.

As anticipated from the form of (22), when $\langle u^2\rangle$ is small α is approximately unity and β is small. As the flow becomes more vigorous the β-term in (22) becomes more important and γ is negative, corresponding to particle accumulation at points where u is small.

Before proceeding to estimation of the Lagrangian displacement r, further discussion of the philosophy and limitations of using estimators like (22) is in order. In defense, it must be said that exact solutions to (21) exist only for the simplest flows and that approximate expansion solutions are defensible only for very restrictive assumptions such as the weak-interaction assumption. The statistical estimator is based on approximate analysis and uses statistical procedures only to optimize the approximate analytic forms which are its foundation. If more accurate analytic approximations for ρ were available it would still be desirable to optimize them according to a statistical measure of error. The improvement of imperfect dynamical models through statistical optimization was discussed briefly by Davis (1977); a graphic example of the utility of the procedure was supplied by Lorenz (1977). Basically, once a measure of error has been defined the statistical optimization of a model can only improve its average accuracy. Unfortunately, it cannot be ensured that the error as measured by another criterion will also be minimized. For example, minimizing at every point the mean square of $d\epsilon/dt$ does not insure the smallest mean square of ϵ; neither does it follow that the ϵ with smallest mean square will yield the most accurate averages in (19) and (20). Thus, while statistical optimization has been shown to greatly enhance imperfect analytic models, success is not assured and efficacy can only be determined through comparison with exact results.

An estimate of the Lagrangian displacement $r(\tau)$ which appears in (20) can be approached through a statistically optimized approximate solution of

$$\frac{dr}{dt} = u(r,t).$$

One such approximation is

$$r(\tau) = \mu(\tau)\, u(x,t) + \nu,$$

with μ selected to minimize the mean square of $d\nu/dt$ and ν treated as a normally distributed random variable independent of u and ρ. When compared with direct simulations (see § 4) it was found that this estimate was in no way superior to the much simpler hypothesis that $r(\tau)$ is an independent normally distributed random variable. Only the simpler estimate will be considered here since it is much easier to implement. As will be seen in the following section, this simple approximation is closely related to Corrsin's conjecture (12) and the parametrized Gaussian model of § 2.5.

3.3. *The estimator model*

Following the procedures outlined above, it is possible to select appropriate values of α, β and γ, thereby specifying the unknowns in (22) or the equivalent

$$\rho = \{[1+\beta u^2]^\gamma e^{-\alpha\eta_x}\}\rho_0^{-1} + \epsilon', \tag{23}$$
$$\rho_0 = \langle [1+\beta u^2]^\gamma e^{-\alpha\eta_x}\rangle,$$

where $\langle\epsilon'\rangle = 0$ and ϵ' is to be treated as a random variable independent of u.

With ρ specified by (23) it is possible to find the mean drift velocity V and the mean-square Lagrangian velocity $\langle v^2\rangle$ directly from (19) and (20), without knowledge of the displacement r. This involves evaluation of averages of the form

$$\langle u^n [1+\beta u^2]^\gamma e^{-\alpha\eta_x}\rangle$$

for $n = 0$, 1 and 2. This could be accomplished through integration using the joint-normal distribution of u and η_x but is made simpler by noting that η_x itself can be specified exactly in terms of u using the minimum-mean-square-error estimator

$$\eta_x = \frac{\langle u\eta_x\rangle}{\langle u^2\rangle} u + \zeta, \tag{24}$$

where

$$\langle\zeta\rangle = \langle u\zeta\rangle = 0, \quad \langle\zeta^2\rangle = \langle\eta_x^2\rangle - \langle u\eta_x\rangle^2/\langle u^2\rangle.$$

Since u and η_x are joint-normally distributed, so are u and ζ; since the latter are uncorrelated it follows that they are independent. Thus

$$V = F_1/F_0, \quad \langle v^2\rangle = F_2/F_0, \tag{25a, b}$$

where

$$F_n = \langle u^n [1+\beta u^2]^\gamma e^{-\alpha^* u}\rangle,$$
$$\alpha^* = \alpha\langle u\eta_x\rangle/\langle u^2\rangle.$$

The constants F_n can be computed by a single integration of the univariate normal distribution of u.

In the limit of weak flows $\alpha \to 1$, $\beta \to 0$ and $\langle u\eta_x\rangle/\langle u^2\rangle^{\frac{1}{2}} \to 0$. In this case (25) reduces to the leading terms of the weak-interaction predictions

$$V = -\langle u\eta_x\rangle = \langle u_x\eta\rangle, \quad \langle v^2\rangle = \langle u^2\rangle.$$

This agreement follows from the fact that the statistical estimator for ρ was chosen so that it could equal the weak-interaction approximation if statistical optimization indicates that $\alpha = 1$ is the optimal choice.

Evaluation of the Lagrangian covariance from (20) is accomplished by noting that when r is approximated as an independent, normally distributed variable

$$\begin{aligned}\langle v(0)\, v(t)\rangle &= \langle \rho(0,0)\, u(0,0)\, u(r,t)\rangle \\ &= \int dx \langle \rho(0,0)\, u(0,0)\, u(x,t)\rangle \langle \delta(x - r\{t\})\rangle \\ &= \int dx \langle \rho(0,0)\, u(0,0)\, u(x,t)\rangle \frac{1}{\sigma\sqrt{(2\pi)}} e^{-(x-\langle r\rangle)^2/2\sigma^2}, \end{aligned} \tag{26}$$

where $\sigma^2 = \langle [r - \langle r\rangle]^2\rangle$. The second line of (26) will be recognized as Corrsin's conjecture modified for the effects of non-uniform particle distribution in the long-after-deployment limit; the third line is the analogue of the parametrized Gaussian model of § 2.5. These two correspondences follow respectively from taking r independent of both ρ and u and from taking r to be normally distributed.

Substitution of the estimators (23) and (24) into (26) followed by evaluation of the average yields

$$\langle v(0)\, v(t)\rangle = \int dx \frac{1}{\sigma\sqrt{(2\pi)}} e^{-(x-Vt)^2/2\sigma^2} [a_2(x,t) F_2 + \alpha a_1(x,t) F_1] \frac{1}{F_0}, \tag{27}$$

where

$$\begin{aligned} a_2(x,t) &= \langle u(0,0)\, u(x,t)\rangle / \langle u^2\rangle, \\ a_1(x,t) &= \langle u\eta_x\rangle a_2 - \langle \eta_x(0,0)\, u(x,t)\rangle. \end{aligned}$$

The space–time-lagged mean products in a_1 and a_2 may be related to the wavenumber–frequency spectrum $\Phi(k,\omega)$ of (1) and the integration in (27) performed. For the special case of an isotropic spectrum with $\Phi(-k,\omega) = \Phi(k,\omega)$ this yields

$$L(t) = \frac{\langle v^2\rangle}{\langle u^2\rangle} \int\int d\omega\, dk\, \Phi(k,\omega)\, e^{-\frac{1}{2}k^2\sigma^2} \cos\omega t. \tag{28a}$$

According to (4)

$$\frac{d^2}{dt^2} \tfrac{1}{2}\sigma^2 = L(t), \tag{28b}$$

which, coupled with the initial conditions $\sigma = d\sigma/dt = 0$ at $t = 0$, forms a single differential equation from which $L(t)$ may be determined.

More elaborate predictors for the displacement $r(t)$ can be employed and lead to differential equations similar to (28) with considerably more complex expressions for $L(t)$ in terms of $\Phi(k,\omega)$. As mentioned in § 3.2, no such extension yet examined has produced better comparison with simulations than that achieved from (28).

4. Comparison with simulations

In this section the foregoing theories are tested through comparison with simulations of particle motion in one dimension. Attention is restricted to the single-particle statistics of mean Lagrangian velocity and the frequency spectrum which itself determines the mean-square Lagrangian velocity and the single-particle 'eddy dispersion' as defined in (4). The philosophy is the same as that of Kraichnan (1970),

who presented the results of simulating particle motion in two and three dimensions, but there are some noteworthy differences. Firstly, anisotropic velocity fields are considered so that non-zero Lagrangian mean velocity can be observed with a vanishing Eulerian mean velocity. Secondly, comparison is made between observed and predicted frequency spectra rather than time-lagged covariances; this permits a more detailed comparison than is possible using plots of covariances which are dominated by energy-containing scales. Thirdly, the Eulerian spectra employed here contain features which accentuate the differences between Eulerian and Lagrangian spectra; in particular, one Eulerian spectrum examined contains no energy at zero frequency so that any 'eddy dispersion' (proportional to the Lagrangian spectrum at zero frequency) results from the nonlinear Eulerian–Lagrangian relation which the theories seek to predict. Additional simulations of particle motion in one dimension are presented by Liu & Thompson (1974).

Simulations are based on stationary, homogeneous, and joint-normally distributed Eulerian velocity fields composed of a spectrum of components obeying the dispersion relation $\omega^2 = k$. The Eulerian wavenumber–frequency spectrum, defined in (1), is

$$\Phi(k,\omega) = \phi(\omega)\,[Q_N \delta(k-\omega|\omega|) + Q_P \delta(k+\omega|\omega|)]. \tag{29}$$

The function ϕ is an even function of ω and the integral of ϕ over positive and negative frequencies is unity; thus the mean-square Eulerian velocity is $Q = Q_N + Q_P$ and Q_N and Q_P are, respectively, the variance associated with waves which propagate in the negative and positive x-directions. The mean Eulerian velocity is always zero. The time and length scales are chosen so that energy in the Eulerian spectrum is limited to $|\omega| \leqslant 1$ and $|k| \leqslant 1$. Thus Q is the ratio of mean-square Eulerian velocity to the square of the propagation velocity of the slowest components with $\omega = k = 1$. Small Q corresponds to wavelike conditions and the limit $Q \to \infty$ is 'frozen turbulence'.

Reported here are results obtained from two Eulerian spectral shapes. These were

$$\phi = \tfrac{1}{2} \quad \text{for} \quad |\omega| < 1$$

and

$$\phi = [2 \ln 5]^{-1} \omega^{-1} \quad \text{for} \quad \tfrac{1}{5} < |\omega| < 1,$$

with $\phi = 0$ unless noted. The first spectrum will be referred to as the 'flat spectrum' and the second as the 'ω^{-1} spectrum'. The spectra were either isotropic, with

$$Q_N = Q_P = \tfrac{1}{2}Q,$$

or unidirectional, with $Q = Q_P$ and $Q_N = 0$.

Realizations of Eulerian velocity fields were generated using eighty independent Fourier components selected using a pseudo-random number generator to have normally distributed amplitudes with variances appropriate to the particular $\phi(\omega)$ used in (29). For each realization, the particle position was determined by integrating (2) with a finite-difference predictor–corrector scheme involving analytic evaluation of Lagrangian velocity and its derivative and leading to a relative error of order time-step cubed.

Primary interest here is in 'long-after-deployment' statistics which are stationary. A transition to stationary statistics was verified for both Eulerian spectra and it was found that the timescale of transition predicted by (5) is characteristic of the approach to stationarity of both V and $\langle v'^2 \rangle$. Long-after-deployment statistics were then

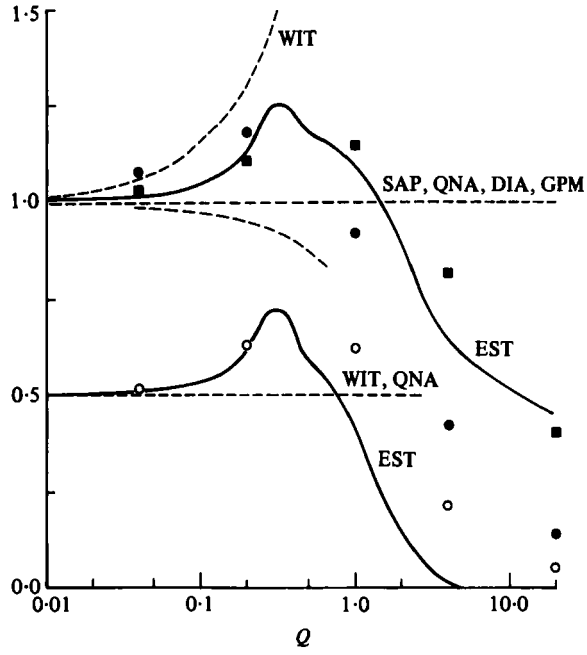

FIGURE 1. Mean and variance of Lagrangian velocity for the ω^{-1} Eulerian spectrum. Upper curves and filled-in symbols are $\langle v'^2 \rangle / Q$, lower curves and open symbols are V/Q. Squares are observations for the isotropic spectrum, circles the unidirectional propagation case. Three-letter identifiers of theories are defined in the text, WIT and DIA variance predictions are the same for isotropic and unidirectional cases. For variance QNA denotes isotropy, QNA→ is the unidirectional case.

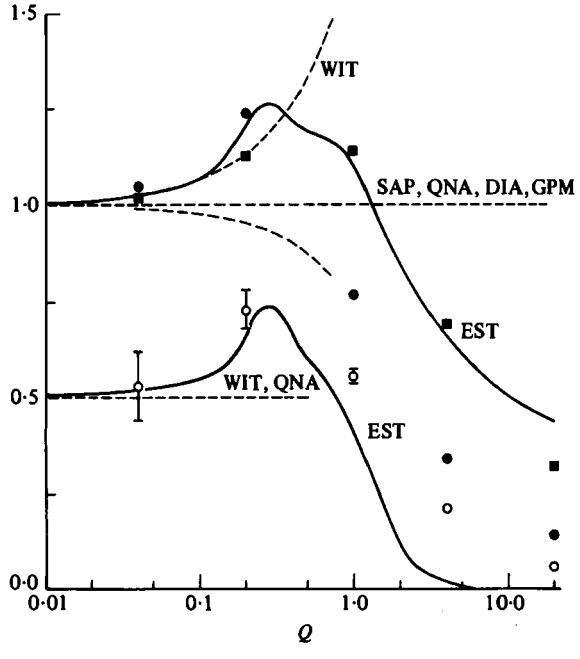

FIGURE 2. As figure 1 but for the flat Eulerian spectrum.

accumulated for $64 < t < 576$, where no lack of stationarity could be detected; for each case examined the histories of 125 particles were used for averaging. The major points of comparison for the theories were the mean Lagrangian drift velocity V, the variance of Lagrangian velocity $\langle v'^2 \rangle$, and the shape of the frequency spectrum of velocity. Examination of multi-particle statistics is deferred for a later report.

In the subsequent discussion the various theories of § 2 and § 3 are referred to by the following shorthand notations: weak-interaction theory of § 2.1, WIT; successive-approximation procedure of § 2.2, SAP; quasi-normal approximation of § 2.3, QNA; direct-interaction approximation of § 2.4, DIA; Gaussian parametrization model of § 2.5, GPM; statistical estimator of § 3, EST.

The normalized mean velocity V/Q and variance $\langle v'^2 \rangle/Q$ for the ω^{-1} spectrum are plotted in figure 1 and those for the flat spectrum are plotted in figure 2. The two figures are remarkably similar, even to the point of showing a consistent pattern of differences of variance between isotropic and unidirectional spectra. At small Q the variance approaches Q (i.e. equal Lagrangian and Eulerian velocity variance) and the drift becomes proportional to Q. In the flat-spectrum case it is difficult to determine V when Q is small because of relatively large variability associated with the zero-frequency energy in the Eulerian spectrum. As Q increases both $\langle v'^2 \rangle/Q$ and V/Q begin to increase and then decline rapidly when Q exceeds unity. This type of behaviour is anticipated as a result of the phenomena of particle trapping at points where $u = 0$, $\partial_x u < 0$ as discussed in § 3.2.

To the order developed in § 2.1, WIT predicts a constant value of V/Q and a value of the difference between Q and $\langle u'^2 \rangle$ which is $O(Q^2)$ and is the same for isotropic and unidirectional spectra. The variation of $\langle v'^2 \rangle/Q$ is accurately described for small Q and the small-Q limit of V/Q is correct. As anticipated for an asymptotic expansion, the predictions become inaccurate unless $Q \ll 1$.

The SAP predicts $\langle v'^2 \rangle + V^2 = Q$ and thus fails to predict the observed variation of $\langle v'^2 \rangle/Q$ for isotropic spectra or the occurrence of $\langle v'^2 \rangle$ greater than Q. As discussed in § 2.2, SAP predicts $V = 0$ in the long-after-deployment limit unless the Eulerian spectrum vanishes at zero frequency and figure 2 shows this to be incorrect.

The QNA predicts the same V as that obtained from WIT and $\langle v'^2 \rangle = Q - V^2$. These are unsatisfactory predictions unless $Q \ll 1$.

The DIA predicts $\langle v'^2 \rangle = Q$, satisfactory for small Q. The DIA evolution equation was not solved so the predictions for V cannot be compared with simulations. As discussed in § 2.4, the predictions of V for small Q are similar to WIT and thus reasonable.

The GPM predicts $\langle v'^2 \rangle + V^2 = Q$ but is not capable of predicting V. Even if exact values of V are used, the variance predictions are unsatisfactory for large Q and do not describe the rise of $\langle v'^2 \rangle/Q$ observed around $Q = 0{\cdot}3$.

The statistical-estimator model provides mean-velocity and velocity-variance predictions which describe quite well the behaviour of a wide range of Q, describing both the rises of $\langle u'^2 \rangle/Q$ and V/Q near $Q = 0{\cdot}3$ and the marked decrease of these variables at large Q. The kink in these predictions near $Q = 5$ is an artifact associated with a singularity in the function $\gamma(Q)$ in (23).

For each Eulerian spectrum the frequency spectrum of the Lagrangian velocity was computed from 125 velocity histories spanning $64 < t < 576$, providing a fundamental frequency resolution of $\Delta\omega = 0{\cdot}0123$. The observed spectra plotted here were

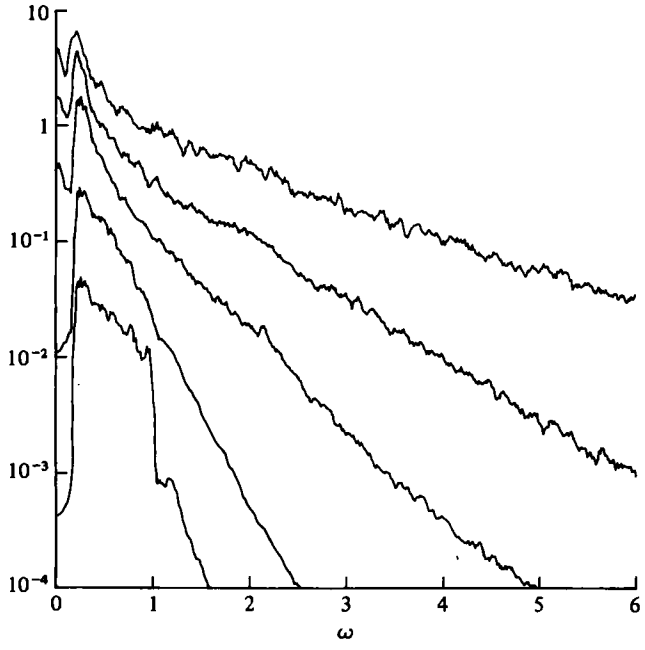

FIGURE 3. Observed frequency spectrum of particle velocity from the isotropic ω^{-1} Eulerian spectrum. The elementary bandwidth is 0·0123, 125 particle histories are averaged and the spectrum is smoothed with a five-point equal-weight running mean. The curves correspond to Q = 0·04, 0·2, 1·0, 4·0, 20·0.

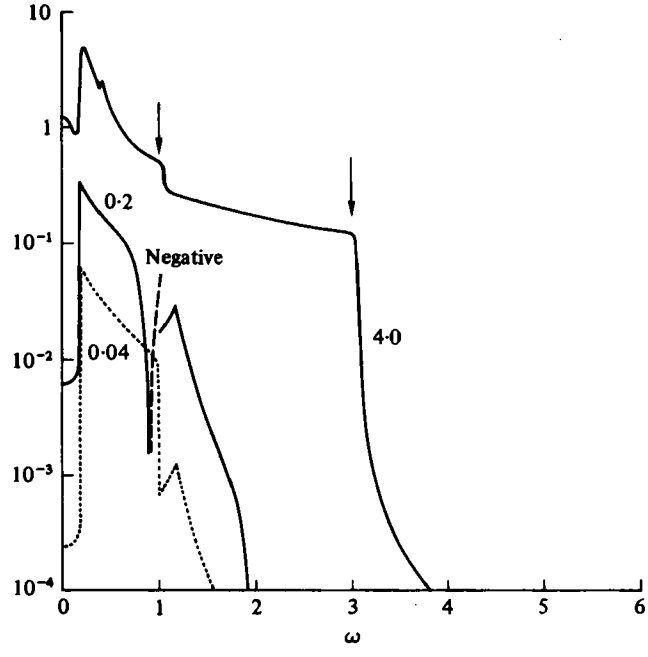

FIGURE 4. Frequency spectra predicted by MIT and QNA for the isotropic ω^{-1} Eulerian spectrum. Lower curves are WIT predictions for Q = 0·04 and 0·2; in the latter negative predictions are shown by a dashed line and there is a discontinuity at ω = 1. The upper curve is the QNA prediction for Q = 4·0; the features marked by arrows are discussed in the text.

smoothed with a five-point, equal-weight running mean. Figure 3 contains Lagrangian spectra obtained from isotropic ω^{-1} Eulerian spectra. Even for $Q = 0{\cdot}04$ the energy outside the frequency range $0{\cdot}2 < \omega < 1$ is a result of differences between Lagrangian and Eulerian spectra, not analysis spreading. As Q increases the spectra show increased transfer to both high and low frequencies so that for $Q > 1$ almost all vestiges of the band-limited nature of the Eulerian spectrum are lost.

Of the theories in § 2 and § 3, two yield unacceptable predictions for the shape of the Lagrangian frequency spectrum and three yield reasonably accurate predictions. The unacceptable spectra are predicted by WIT and QNA, those theories of § 2 which were capable of estimating Lagrangian drift. Both SAP and GPM yield acceptable spectral estimates but fail to predict mean drift while EST yields both acceptable drifts and spectra.

Examples of the unsatisfactory nature of WIT and QNA spectral predictions are shown in figure 4 where Lagrangian spectra for the symmetric ω^{-1} Eulerian spectra are shown.

The WIT prediction for $Q = 0{\cdot}04$ strongly resembles the observed spectrum in figure 3 but the $Q = 0{\cdot}2$ spectrum shows only a weak resemblance to the general shape of the observed spectrum and, over a range of frequencies, contains physically unrealizable negative spectral values. As the value of Q increases above $0{\cdot}2$ the region of frequencies over which the predicted spectrum is negative increases and the overall spectral shape becomes less realistic, primarily because the variance is confined to $\omega < 2$. As a general rule, for $0{\cdot}2 < \omega < 2$ WIT exaggerates the difference between Eulerian and Lagrangian spectra so that where the true Lagrangian spectrum is lower than the Eulerian the prediction can become negative. Energy is limited to $\omega < 2$ because the theory is carried only to third order, thus including only interaction triads in which two members are first-order components with frequencies less than unity. Thus the highest-frequency component is the 'sum frequency' component with frequency less than 2.

The QNA-predicted spectra are somewhat more realistic than those from WIT. For $Q < 0{\cdot}1$ the predictions are reasonable but as Q increases the spectral shapes become completely unrealistic, as evidenced by the $Q = 4$ example in figure 4. Consistent features of QNA spectra for $Q \geqslant 1$ are a maximum energetic frequency $\omega = 1+\sqrt{Q}$ and an abrupt energy decrease at $\omega = 1-\sqrt{Q}$; these are indicated by the two vertical arrows in figure 4. It will be recalled from § 2.3 that the early-time behaviour of the particle concentration is characterized as a wave of propagation speed $\sqrt{Q}$. Thus the $\omega = 1 \pm \sqrt{Q}$ features, of which there is no indication in the observations, would appear to be spurious artifacts of particles 'propagating' at speed $\sqrt{Q}$ through the slowest-moving Eulerian velocity components with $\omega = k = 1$.

Figure 5 depicts the SAP spectral predictions and observed spectra for various values of Q in the symmetric ω^{-1} Eulerian spectrum. The predictions for $Q < 1$ are remarkably accurate. The general behaviour of the observed spectra with increasing Q is reproduced but there is a consistent overestimate of high-frequency energy and the features around $\omega = 0{\cdot}2$ are smoothed away more completely than is observed. Nevertheless, the predictions of spectral shape are credible, particularly when it is noted that some of the discrepancy in figure 5 seen for $Q > 1$ is the result of SAP overestimating the Lagrangian variance.

Figure 6 depicts the statistical-estimator spectral predictions for the same ω^{-1}

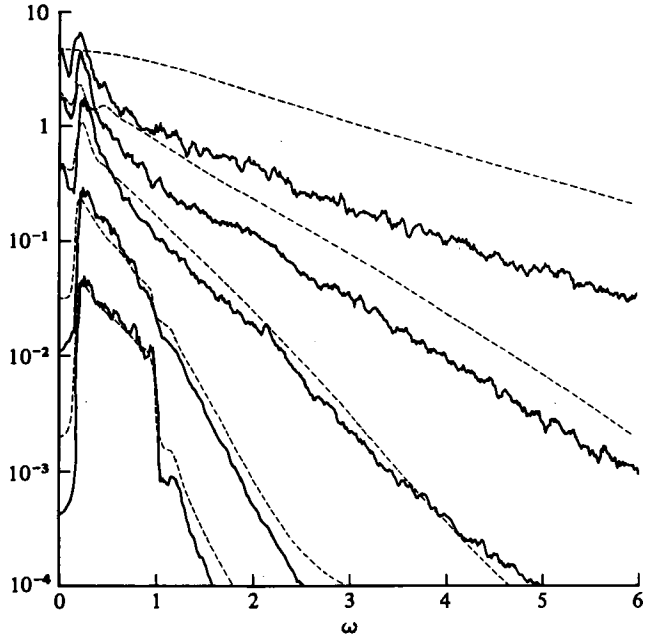

FIGURE 5. Frequency spectra predicted by SAP superposed on observations from figure 3.

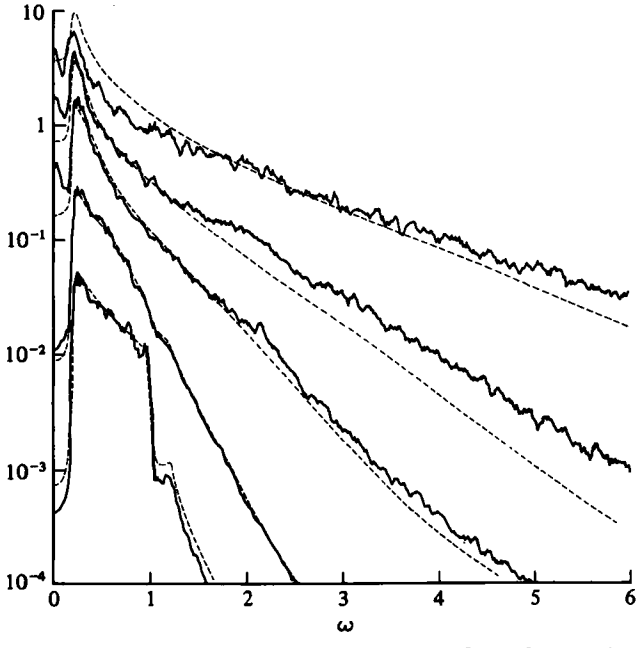

FIGURE 6. Frequency spectra predicted by EST superposed on observations from figure 3. The three lower curves for Q = 0·04, 0·2, 1·0 are also GPM predictions and the upper two are very similar to their GPM counterparts.

spectrum as figure 5. As discussed in § 3, there is considerable similarity between the spectral estimates of EST and GPM. In fact, as (28*a*) shows, when the Eulerian spectrum is symmetric the two forms differ only by a constant factor. Thus the reasonable agreement between simulation and prediction found in figures 6 and 7 (the spectral predictions for the flat spectrum) demonstrates that both EST and GPM are useful for predicting spectral shape.

For reasons mentioned above, no DIA spectral predictions were computed for comparison with the one-dimensional simulations. Kraichnan (1970) did compare observed Lagrangian velocity correlation functions with those predicted by DIA for two- and three-dimensional flows. When SAP, GPM and EST predictions for the one-dimensional spectra examined here are compared with observed correlation functions the degree of similarity is similar to what Kraichnan found for his '$\omega_0 = v_0 k_0$' cases and better than he found for the frozen-turbulence '$\omega_0 = 0$' cases. Unfortunately, Kraichnan's correlation-function plots do not permit a very precise comparison so that one can only say that DIA, like SAP, GPM and EST, produces credible spectral predictions. It should be noted that Lundgren & Pointin (1976) compared the correlations predicted by GPM with Kraichnan's results and found an agreement with observations which was comparable to that obtained by the much more complicated DIA predictions.

5. Summary

The intent of this work was to determine which of several theoretical approaches led to good predictions of the Lagrangian velocity statistics describing motion of single particles in stationary and homogeneous velocity fields. It was felt that this was the appropriate first step before proceeding to examine more complex questions such as the dispersion of particle clouds or the effects of Eulerian fields whose statistics vary in space.

Toward this end the theories of § 2 (WIT, SAP, QNA, DIA and GPM) were examined first. It was noted that these theories could be divided into categories depending on whether they were based on exact averaging of approximate solutions of the kinematic equation (WIT and SAP) or on exact solutions of equations hypothesized to describe the evolution of statistical properties (QNA, DIA and GPM). Of these theories DIA is the most complicated to implement and was not compared with simulations. From the discussion of § 2.4 it is evident that DIA leads to plausible estimates of the Lagrangian mean drifts and, from Kraichnan's (1970) results, it is known that it yields good predictions of the frequency spectrum of particle velocity. The other theories, however, have unacceptable features. WIT and QNA produce poor frequency-spectrum estimates, SAP and GPM cannot predict mean drifts in anisotropic velocity fields, WIT yields reasonable Lagrangian velocity-variance estimates only for weak wavelike flows, and no theory explains the observed variation of Lagrangian velocity variance as the strength of the flow varies from wavelike to strongly nonlinear.

In retrospect these conclusions could, in large measure, be anticipated. Weak-interaction theory is an asymptotic expansion about the weak-flow limit and therefore could not be expected to yield useful results for flows where particle velocities are comparable with the phase velocities of Eulerian velocity components. This may explain why WIT has therefore been used only to predict mean Lagrangian velocity

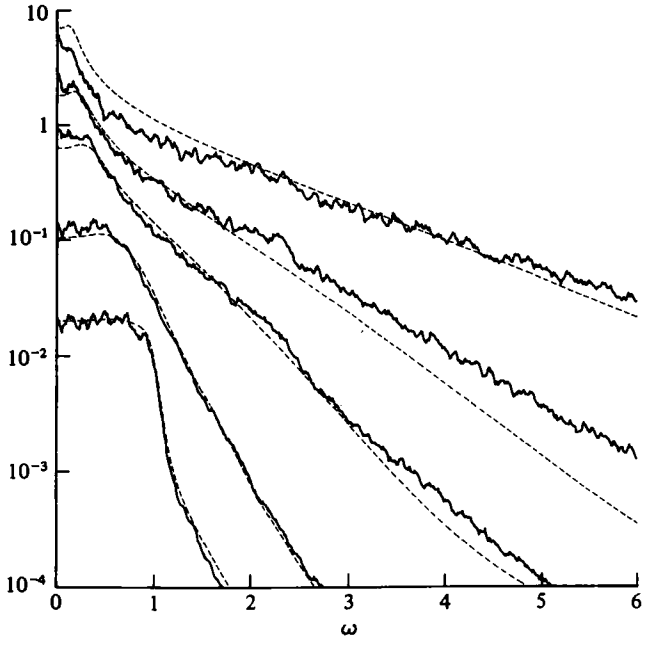

FIGURE 7. Observed particle velocity spectra from the isotropic flat Eulerian spectrum for Q = 0·04, 0·2, 1·0, 4·0, 20·0 (solid curve) and corresponding EST predictions (dashed).

(Stokes drift) but also serves as a cautionary note with regard to the use of WIT in predicting the spectral evolution of nonlinear systems as is done by Hasselman (1966). The other theories all suffer to some degree from failing to account for the difference between initial and late-time behaviour of randomly deployed particles. This explains why SAP and GPM do not describe mean drift, which depends on development of relations between particle position and the velocity at that point. Similarly, failure to account for the difference between initial and long-after-deployment statistics leads SAP, QNA and GPM to predict equal mean squares of the Lagrangian and Eulerian velocities.

In an attempt to avoid the inadequacies of WIT, SAP, QNA and GPM while maintaining an equivalent computational simplicity and clarity of physical hypothesis, neither of which is found in DIA, the statistical-estimator theory of § 3 was developed. The approach is unique in that approximate solutions of the kinematic equation are developed on the basis of minimizing the mean-square error in that equation rather than on a prescribed expansion or iteration procedure such as employed in WIT and SAP. In its simplest form, only the first weak-interaction correction to particle density (the α-term in (23)) is employed and the particle position is taken as unpredictable. This leads to reasonable mean drift estimates and, for isotropic spectra, Lagrangian-spectrum predictions which are identical to those of GPM, the most accurate spectral predictor examined in § 2. In some sense the virtue of EST is its ability to predict mean drift as accurately as WIT and QNA while equalling the spectral predictions of GPM which are as accurate as any theory examined, including DIA. Further, by including the phenomenon of particle-trapping into the approximate solution (the β-term in (23)) one obtains a prediction of the varying ratio of Lagrangian to Eulerian velocity variance as the strength of the flow increases. It is surprising that EST

spectral predictions are not improved by using more accurate approximations of particle displacement than the 'unpredictable' form used in (26). This substantiates the utility of Corrsin's conjecture (12) which is employed in QNA, DIA and GPM.

While no theory yet predicts accurately Lagrangian velocity statistics, the statistical-estimator model does describe the major features of single-particle Lagrangian statistics. It may be hoped, then, that the model may fruitfully be employed in the examination of multi-particle statistics and Eulerian flow fields more complex than the one-dimensional, homogeneous, joint-normally distributed case examined here.

This work was supported by Office of Naval Research under contract N00014-75-C-0152. I wish to thank R. Kraichnan for helpful suggestions and corrections added in review.

REFERENCES

ABRAMOWITZ, M. & STEGUN, I. A. 1964 *Handbook of Mathematical Functions*, Chap. 7. Nat. Bureau of Standards, Washington, D.C.

CORRSIN, S. 1960 Progress report on some turbulent diffusion research. In *Proc. Symp. on Atmospheric Diffusion and Air Pollution*, pp. 161–164. Academic.

DAVIS, R. E. 1977 Techniques for statistical analysis and prediction of geophysical fluid systems. *Geophys. Astrophys. Fluid Dyn.* **8**, 245–277.

HASSELMAN, K. 1966 Feynman diagrams and interaction rules of wave–wave scattering processes. *Rev. Geophys. Space Phys.* **4**, 1–32.

HINZE, J. O. 1959 *Turbulence*, Chap. 5. McGraw-Hill.

HOULT, D. P. 1968 Euler-Lagrange relationship for random dispersive waves. *Phys. Fluids* **11**, 2082–2086.

KENYON, K. E. 1969 Stokes drift for random gravity waves. *J. Geophys. Res.* **74**, 6991–6994.

KRAICHNAN, R. H. 1959 The structure of isotropic turbulence at very high Reynolds numbers. *J. Fluid Mech.* **5**, 497–543.

KRAICHNAN, R. H. 1965 Lagrangian-history closure approximation for turbulence. *Phys. Fluids* **8**, 575–598.

KRAICHNAN, R. H. 1970 Diffusion by a random velocity field. *Phys. Fluids* **13**, 22–31.

KRAICHNAN, R. H. 1977 Lagrangian velocity covariance in helical turbulence. *J. Fluid Mech.* **81**, 385–398.

LIU, H. & THOMPSON, R. 1974 Conversion of Eulerian to Lagrangian statistics in one dimension. *Utilitas Math.* **10**, 109–128.

LORENZ, E. N. 1977 An experiment in nonlinear statistical weather forecasting. *Mon. Wea. Rev.* **105**, 590–602.

LUNDGREN, T. S. & POINTIN, Y. B. 1976 Turbulent self-diffusion. *Phys. Fluids* **19**, 355–358.

PHILLIPS, O. M. 1977 *The Dynamics of the Upper Ocean*. Cambridge University Press.

PHYTHIAN, R. 1975 Dispersion by random velocity fields. *J. Fluid Mech.* **67**, 145–153.

RICHARDSON, L. F. 1926 Atmospheric diffusion shown on a distance–neighbour graph. *Proc. R. Soc. Lond.* A **110**, 709–727.

ROBERTS, P. H. 1961 Analytical theory of turbulent diffusion. *J. Fluid Mech.* **11**, 257–283.

SAFFMAN, P. G. 1962 An approximate calculation of the Lagrangian autocorrelation coefficient for stationary homogeneous turbulence. *Appl. Sci. Res.* A **11**, 245–255.

SAFFMAN, P. G. 1969 An application of the Weiner–Hermite expansion to diffusion of a passive scalar in a homogeneous turbulent flow. *Phys. Fluids* **12**, 1786–1798.

STOMMEL, H. 1949 Horizontal diffusion due to oceanic turbulence. *J. Mar. Res.* **8**, 199–225.

TAYLOR, G. I. 1921 Diffusion by continuous movements. *Proc. Lond. Math. Soc.* **20**, 196–212.